

Article

Impact of Climate Change on the Energy and Comfort Performance of nZEB: A Case Study in Italy

Serena Summa ^{*}, Luca Tarabelli , Giulia Ulpiani and Costanzo Di Perna

Industrial Engineering and Mathematical Sciences Department, Università Politecnica delle Marche, via Brecce Bianche 1, 60131 Ancona, Italy; l.tarabelli@univpm.it (L.T.); giuliaulpiani@gmail.com (G.U.); c.diperna@univpm.it (C.D.P.)

* Correspondence: s.summa@pm.univpm.it

Received: 2 October 2020; Accepted: 26 October 2020; Published: 2 November 2020



Abstract: Climate change is posing a variety of challenges in the built realm. Among them is the change in future energy consumption and the potential decay of current energy efficient paradigms. Indeed, today's near-zero Energy buildings (nZEBs) may lose their virtuosity in the near future. The objective of this study is to propose a methodology to evaluate the change in yearly performance between the present situation and future scenarios. Hourly dynamic simulations are performed on a residential nZEB located in Rome, built in compliance with the Italian legislation. We compare the current energy consumption with that expected in 2050, according to the two future projections described in the Fifth Assessment Report (AR5) by the Intergovernmental Panel on Climate Change (IPCC). Implications for thermal comfort are further investigated by assuming no heating and cooling system, and by tracking the free-floating operative temperature. Compared to the current weather conditions, the results reveal an average temperature increase of 3.4 °C and 3.9 °C under RCP4.5 and RCP8.5 scenarios, estimated through ERA-Interim/UrbClim. This comes at the expense of a 47.8% and 50.3% increase in terms of cooling energy needs, and a 129.5% and 185.8% decrease in terms of heating needs. The annual power consumption experiences an 18% increase under both scenarios due to (i) protracted activation of the air conditioning system and (ii) enhanced peak power requirements. A 6.2% and 5.1% decrease in the hours of adaptive comfort is determined under the RCP4.5 and RCP8.5's 2050 scenarios out of the concerted action of temperature and solar gains. The results for a newly proposed combined index for long-term comfort assessments reveal a milder future penalty, owing to less pronounced excursions and milder daily temperature swings.

Keywords: climate change; near-zero energy buildings; future scenarios; energy efficiency; adaptive comfort; long-term performance

1. Introduction

CO₂ emissions are causing a prolonged and clear increase in global temperatures [1]. In 2010, the building sector accounted for about 32% of global energy consumption, 19% of CO₂ emissions and 51% of global electricity consumption [1]. If, on one side, buildings and their related activities are responsible for a significant portion of greenhouse gas emissions, on the other side they represent a great opportunity for mitigation and adaptation to climate change effects [2].

In order to limit the temperature increase to 2 °C compared to pre-industrial levels, the Fifth Assessment Report (AR5) by the Intergovernmental Panel on Climate Change (IPCC) considers four different future scenarios (RCP; Representative Concentration Pathways) which show how the climate will likely change by 2100, depending on different levels of counteraction [3]. When bold mitigation strategies are taken into consideration, the greenhouse gas emissions could be halved by 2050 with a maximum temperature increase of 2 °C, while, with a “business-as-usual” approach, the CO₂ in the

atmosphere would increase fourfold compared to pre-industrial levels, with temperature differences exceeding 4 °C. The corresponding change in global and local climatic conditions will impact the energy needs of the existing building stock and, consequently, the primary energy demand [3].

Speaking of buildings and climate change, two main aspects are highlighted in the literature: (i) the assessment of the repercussions in different geographical areas and for different uses of the built space, and (ii) the development of a broad spectrum of techniques to enhance buildings' resilience (no nZEB) and thus mitigate the energy penalty associated with climate change.

Regarding the first point, many studies in the literature report on the major impact of climate change on buildings. For instance, Ciancio et al. [4] compared the current energy needs of a residential building in the context of 19 different European cities, with those expected in 2080. The results show an increase in energy needs for cooling of up to 272% in Mediterranean cities, and a decrease in energy needs for heating up to 45% in Northern European countries. In the same vein, Olonscheck et al. [5] used projections of the regional statistical climate model STAR II and demonstrated that the energy demand for air conditioning in a residential building in Germany will decrease during winter, while remaining almost constant during summer for the next 40 years.

In Chile, Verichev et al. [6] described how temperature increases of 0.68 °C (under RCP2.6) and 1.51 °C (under RCP8.5) will lead to decreases in annual heating degree-days of about 72% and 92% by 2065, respectively. Moreover, Angeles et al. [7] predicted increases in energy demand of 9.6 and 23 kWh/month per person in Southern Greater Antilles and the inland of South America, which will lead to increases in cooling loads of 7.57 GW (under RCP2.6) and 8.15 GW (under RCP8.5) by the end of the 21st century.

Other than residential buildings, those with glass surfaces and predominant internal gains will be the ones which will suffer most from the effects of climate change, i.e., offices and schools, where, according to Frank T. [8], cooling energy demand will be up to 1050% higher than the present one for the RCP 8.5 scenario.

In order to contribute to climate change mitigation and, at the same time, tackle the increase in primary energy demand, new buildings are expected to implement not just appropriate envelope designs [9], but also energy production systems from renewable sources, thermal and/or electrical storage systems [10] or passive solar systems [11]. Differently, several strategies will need to be introduced for existing buildings, such as: (i) the installation of more efficient heating, ventilation and air conditioning (HVAC) systems [12,13], (ii) the installation of adequate solar shading, [8] and/or (iii) proper night ventilation [14].

Indeed, beyond materials [15], technology is another key ingredient in nZEB design. Typically, a hybrid combination of active and passive technologies realizes nZEB-like performances. Among the emerging renewable energy-based solutions are micro cogeneration systems, such as fuel cells, photovoltaic thermal, solar thermal reversible heat pump/organic Rankine cycles and cogeneration solar thermoelectric generators [16]. These hybrid systems may also be empowered with load-sharing concepts [17] and advanced energy storage systems based on integrated phase change materials [18] and optimized schedules [19,20]. On a general note, finding the most appropriate matching between envelope features and HVAC system configurations is pivotal, just like working on demand-driven energy flows, the reduced primary energy uptake and the electricity consumption of auxiliaries, such as pumps and fans. Heat pumps are gaining ground owing to their versatility [21] and technological variety [22]. For instance, the use of polyvalent heat pumps or variable air volume systems [23] possibly mated with grid-tied photovoltaic (PV) systems [24] has proven efficient in reducing the overall energy consumption of buildings. Further, heat recovery systems (from sensible heat exchangers up to run around coils or enthalpy, sensible assisted systems by indirect adiabatic cooling) may be implemented with additional perks [23]. Solar energy systems and passive solar concepts are being increasingly used and refined through optimized control systems based on advanced solar irradiance forecasting models [25] and dynamic occupancy profiles [26]. Solar-based advanced technologies include compact collectors for polygenerative applications, high concentrating PV systems [27], and building integrated

photovoltaic systems (BIPV) that not only generate electrical energy but also behave like skin for the buildings [28]. These technologies have the potential to become a source of income for the buildings, even without subsidies, due to the increasing efficiency and decreasing costs of PV systems [29]. Smart management through building control and automation systems is also key, as demonstrated by the introduction of the Smart Readiness Indicator with the latest revision of the EPBD in July 2018 [30]. This applies to any technical systems [31] and to ventilation strategies [32]. Innovative lines of research are further looking into refrigerant-free cooling appliances based on caloric materials [33] and year-round passive daytime radiative cooling [34].

Generally speaking, whatever the specific strategy, the results emphasize that a one-fits-all recipe for nearly-zero energy buildings does not exist [26]. Climate, among other factors, calls for the resolution of diversified optimization problems [35,36]. Climate is a spatial and temporal variable. Here, we focus on the temporal variability by challenging established nZEB paradigms in the context of increased global warming.

Concerning the method, the need to reduce global energy consumption and CO₂ emissions has induced the European Committee for Standardization (CEN) to provide an hourly dynamic calculation method that allows buildings' consumptions to be assessed in a more realistic and detailed evaluation, especially during the summer season [37]. This method, described in EN ISO 52016-1:2017 [38], replaces the one described in ISO 13790:2008 [39] by introducing a new methodology to calculate energy needs for heating and cooling, on both an hourly and a monthly basis.

The need for knowledge on future scenarios emerges, specifically about a better understanding of the most effective energy retrofit strategies for existing nZEB buildings in the Mediterranean climate, to guide future legislative amendments, and the identification of which mitigation policies will be most appropriate for new buildings to limit both CO₂ production and global energy consumption.

Therefore, this study aims at assessing the impact of climate change on (i) the heating and cooling consumption of an nZEB multi-family house, located in Rome and designed according to the most recent Italian regulations [40], and (ii) the level of comfort achieved indoors.

The EURO-CORDEX5 [41] models combined with the ERA-Interim/UrbClim model [42,43], used for predicting future scenarios according to the Fifth Assessment Report (AR5) by the Intergovernmental Panel on Climate Change (IPCC), shows that Rome is the place with the highest temperature increase in Italy; therefore, this city has been chosen as a case study for the present study.

To this end, hourly dynamics simulations were performed in TRNSYS, which is a well-established building dynamic simulation software worldwide, capable of fine assessments of both energy and comfort levels [44], thanks to a vast variety of components that can be implemented in different models in order to simulate a wide range of simple to complex systems [45]. Its visual interface, which implements a component-based approach and the possibility of the addition of new mathematical sub-models, motivates its use for building energy simulation (BES) [46].

The rest of the paper is structured as follows: in Section 2, we present methods; in Section 3, we show the results of the simulations and, in Section 4, we draw conclusions and discuss future work.

2. Methods

In this work, the dynamic simulation software TRNSYS [47] was chosen to assess the thermal behavior of a building located in Rome classified as a nearly-zero energy building (nZEB) according to the Italian regulation enforced on an hourly basis. The focus is on the effects of the expected climate change and urban heat island exacerbation by 2050, both in terms of energy needs and comfort.

To this end, hourly dynamic simulations were performed in TRNSYS according to the following procedure: (i) the production of current and 2050 meteorological input files, (ii) simulations and evaluation of the year-round energy consumption, assuming an infinite power system for heating and cooling, (iii) simulations and evaluation of the free-floating operative temperature assuming no heating/cooling systems, (iv) application of the adaptive comfort [48] theory to rate the quality of the indoor environments and (v) evaluation of the long-term thermal comfort [49].

2.1. Climate and Geographical Data

The hourly climate data of the typical year adopted in this study refer to both the current climate conditions and those in 2050. About future scenarios, two Representative Concentration Pathways (RCPs) were analyzed, which refer to climate change projections developed in the AR5 report by IPCC.

The two future projections (RCP8.5 and RCP4.5) compute the expected temperature rise as a function of different greenhouse gas emissions determined by both human activities and different mitigation activities implemented by local policies:

- RCP8.5 represents a 'business-as-usual' approach, which considers that atmospheric concentrations of CO₂ will triple or quadruple by 2100 compared to pre-industrial levels, thus increasing the air temperature by about 4 °C;
- RCP4.5 contemplates control measure to curtail the greenhouse emissions, assuming a trend reversal (decrease below current levels) by 2070. Consequently, the atmospheric concentrations of CO₂ will be about twice as high as pre-industrial levels by 2100. The increase in air temperature will be capped at 2 °C.

Therefore, three typical annual weather data were retrieved from Meteonorm 7.3 [50]: (i) current climate conditions, (ii) 2050–RCP8.5 climate conditions, and (iii) 2050–RCP4.5 climate conditions.

The current climatic data are developed in a data set of temperatures and solar irradiances measured between 2000 and 2009 and 1991 and 2009, respectively, while future scenarios are simulated by Meteonorm 7.3 through a set of EURO-CORDEX5 [41] models combined with the ERA-Interim/UrbClim model [42,43]. The evaluation of the increase in solar radiation is based on the IPCC AR4 A2 models for CPR 8.5 and A1B for CPR 4.5 [51].

In detail, EURO-CORDEX is the European branch of the CORDEX initiative and produces ensemble climate simulations based on multiple dynamical and empirical-statistical downscaling models forced by multiple global climate models from the Coupled Model Intercomparison Project Phase 5 (CMIP5) [41]. The major aims of the CORDEX initiative are to provide a coordinated model evaluation framework, a climate projection framework, and an interface to the applicants of the climate simulations of climate change impact, adaptation, and mitigation studies [52].

The ERA-Interim/UrbClim model allows you to evaluate the intensity of urban heat of any city in the world with a resolution up to 100 m, providing the necessary input data from international satellite-based land cover, vegetation and soil sealing data and meteorological databases [42,43].

In order to perform simulations through TRNSYS, the following input data were considered: (i) latitude, (ii) dry-bulb external temperature, (iii) relative humidity, and (iv) solar global irradiance on the horizontal plane. Data were provided by the WMO weather station #162390 located in Rome/Ciampino. At 41.8° N (latitude), 12.58° E (longitude) and 131 m above sea level (altitude), the location features a temperate climate, specifically Csa (Mediterranean hot summer climate), in accordance with the Köppen–Geiger climate classification system.

2.2. TRNSYS Model Simulation

Outdoor air temperature, relative humidity and global solar irradiance on the horizontal plane for each of the three different scenarios described in Section 2.1 were provided as inputs through TRNSYS component Type 9 (data reader). Then, these data were transferred to Type 16c, a solar radiation processor which implements the Reindl and Perez 1990 models to obtain beam and diffuse solar irradiances on horizontal and tilted surfaces, respectively. The virtual model of the nZEB case-study was designed through a SketchUp [53] plugin for creating the multi-zone building envelope (TRNSYS3d) [54], and then was provided as input in TRNSYS [47]. Each room of the building was defined by creating a thermal zone for each of them. An interface for the detailed TRNSYS multi-zone building (TRNBuild/Type56) was used for modeling walls, gains and ventilation profiles. In order to comply with the Italian regulation for nZEBs [40], overhangs were integrated to reduce solar gains; therefore, Type 34 was used. An hourly basis zone-by-zone calculation was performed, the results of

which in terms of energy needs and indoor operative temperatures were plotted via Type 65. Figure 1 displays the flowchart.

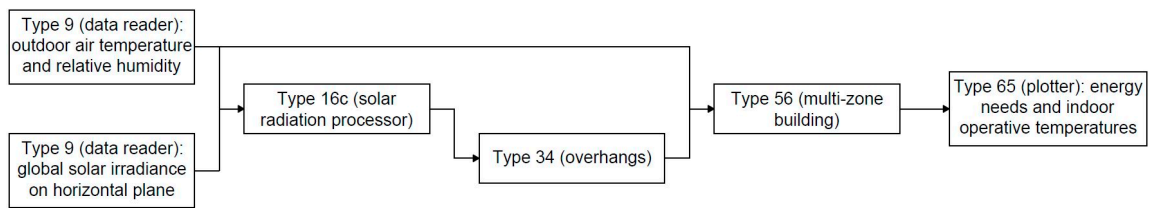


Figure 1. TRaNsient SYstem Simulation (TRNSYS) model flowchart.

2.3. Case-Study

The studied building is a new 3-floor residential nZEB, composed of two apartments per floor. Each apartment has an open space that combines kitchen and living room, a double bedroom, a single bedroom and a bathroom, as shown in Figure 2. Table 1 summarizes the geometrical features of each apartment.

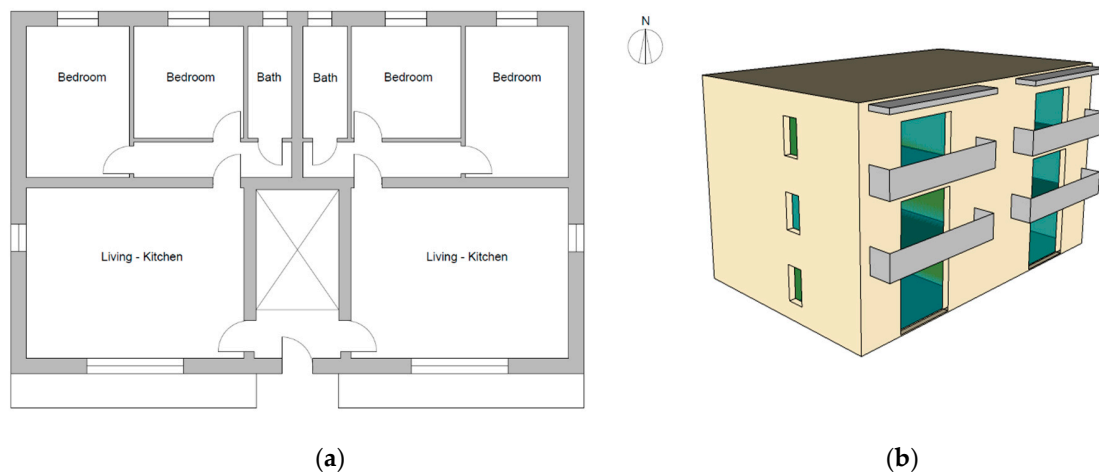


Figure 2. (a) Analyzed building: building plan (1:200) and (b) southwest view.

Table 1. Geometrical features of the apartment.

	Unit	Value
Net floor area	m ²	63.73
Net height	m	2.70
Net volume	m ³	172.07
Window-to-wall ratio	%	15

In order to comply with the Italian nZEB requirements the building envelope is made of 2 cm of external plaster, 35 cm of pored bricks, 4 cm of external insulation, and 1 cm of internal render. The 24 cm hollow-core concrete slab of the flat and non-walkable roof is well insulated with 10 cm of expanded polystyrene. The stairwell wall is made of two layers of 12 cm hollow bricks separated by 6 cm of insulation and external plaster, while the partition wall between the two apartments is a cavity wall with two layers of 12 cm of hollow bricks and external plaster. The windows are double glazed with low-emissivity glass. The horizontal overhangs on the south-exposed facades and proper shading devices on all the windows are modeled in order to provide sufficient sunlight control and the reduction of solar gains. The thermo-physical parameters of the main building envelope elements, previously described, are given in Table 2, while in Table 3 the nZEB requirements for the Italian territory are described.

Table 2. Thermo-physical parameters of building envelope elements.

	Thermo-Physical Parameter	Unit	Value
External wall	Thermal transmittance (U)	W m ⁻² K ⁻¹	0.30
	Internal areal heat capacity (k1)	kJ m ⁻² K ⁻¹	41.70
	External areal heat capacity (k2)	kJ m ⁻² K ⁻¹	19.00
	Periodic thermal transmittance (Yie)	W m ⁻² K ⁻¹	0.013
	Time shift (Δt)	h	17.72
Stairwell wall	Thermal transmittance (U)	W m ⁻² K ⁻¹	0.30
	Internal areal heat capacity (k1)	kJ m ⁻² K ⁻¹	44.90
	External areal heat capacity (k2)	kJ m ⁻² K ⁻¹	44.90
	Periodic thermal transmittance (Yie)	W m ⁻² K ⁻¹	0.048
	Time shift (Δt)	h	13.48
Separating wall between two apartments	Thermal transmittance (U)	W m ⁻² K ⁻¹	0.59
	Internal areal heat capacity (k1)	kJ m ⁻² K ⁻¹	45.00
	External areal heat capacity (k2)	kJ m ⁻² K ⁻¹	45.00
	Periodic thermal transmittance (Yie)	W m ⁻² K ⁻¹	0.148
	Time shift (Δt)	h	11.58
Roof	Thermal transmittance (U)	W m ⁻² K ⁻¹	0.27
	Internal areal heat capacity (k1)	kJ m ⁻² K ⁻¹	65.70
	External areal heat capacity (k2)	kJ m ⁻² K ⁻¹	7.40
	Periodic thermal transmittance (Yie)	W m ⁻² K ⁻¹	0.037
	Time shift (Δt)	h	11.53
Window	Thermal transmittance (U)	W m ⁻² K ⁻¹	1.80
	Solar heat gain coefficient (SHGC)	-	0.71

Table 3. Standard nZEBs energy assessment for the considered case studies.

	Unit	
Energy performance indicator for heating (EP _{H,nd})	[kWh m ⁻²]	5.32
Energy performance indicator for cooling (EP _{C,nd})	[kWh m ⁻²]	28.60
Global average heat transfer coefficient (H _t)	[W m ⁻² K ⁻¹]	0.37
Equivalent solar area/Floor area (A _{sol,est} /A _{sup,utile})	-	0.013

According to the Italian technical specifications in UNI/TS 11300 [55], the following assumptions were made: usage profiles 24/24 h, internal heat gains rate at 5.72 W/m² and ventilation rate at 0.5 h⁻¹. Two different models of the building were created:

- The first one was equipped with an infinite power system for heating and cooling, to evaluate the energy consumption. In this case, the operative temperature, used to control the system, was set to 20 °C in winter and 26 °C in summer, in accordance with the type of building and categories identified in UNI EN 16798-1-Annex A [48], assuming category II as the reference;
- The second one was equipped without any heating and cooling system, to allow free-floating operative temperature for the assessment of thermal comfort. The level of thermal comfort was analyzed through two different approaches. Firstly, we applied the adaptive method, according to which the operative temperatures are compared to the indoor operative temperature ranges defined in UNI EN 16798-1-Annex A [48] for buildings without mechanical cooling systems to identify different comfort levels as a function of the outdoor running mean temperature, calculated as follows:

$$\theta_{rm} = (1 - \alpha) \cdot \{ \theta_{ed-1} + \alpha \cdot \theta_{ed-2} + \alpha^2 \theta_{ed-3} \} \quad (1)$$

In Equation (1), α is a constant between 0 and 1 (recommended value is 0.8) and θ_{ed-i} is the daily mean outdoor air temperature on the i -th previous day.

Secondly, we calculated a newly proposed long-term comfort index (Equation (2)). It outperformed the other 6 types of existing indices (23 total) found in the standards and 5 types of new indices (36 total) for comfort assessments in the long run in a recent comparative study [49]. The correlation with the long-term thermal satisfaction of building occupants was based on continuous thermal comfort measurements and post-occupancy evaluation surveys, but in air-conditioned office buildings. Despite the different casuistry, this combined index proved better at taking into account the triggers behind long-term comfort, namely the pronounced excursions beyond some acceptable temperature ranges and the larger variations in daily temperature than the average experience over time [49]. As such, it is worth investigating its expected variation in future scenarios. This combined, normalized percent index is calculated as follows:

$$index = \left(\frac{\% \text{ To outside specified ranges} + \% \text{ To daily range} > \text{a threshold}}{2} \right) \quad (2)$$

In this study, the hourly operative temperature range was set between 20 °C and 26 °C, in accordance with the type of building and categories identified in UNI EN 16798–1–Annex A [48], assuming category II as reference, and the daily threshold was set to the 80th percentile of the entire simulated database.

3. Results

In this section the modeling results are illustrated and discussed. They refer to the two apartments at the second floor of the building described in Section 2.3. Considering the dispersing surface of the roof, the second floor is the most responsive to external climatic variations. For this reason the results obtained for this floor are evaluated and discussed.

In Section 3.1, the results in terms of kWh obtained from the modeling of the building in the presence of a heating/cooling system are analyzed, while in Section 3.2 the results in terms of comfort obtained with the modeling of the building in free-floating are discussed.

3.1. Simulations to Assess the Energy Consumption

Based on dynamic hourly simulations, the average annual increases in outdoor temperatures (+3.4 °C under RCP4.5 and +3.9 °C under RCP8.5) were found to enhance the global energy consumption from 5079 kWh × year (in 2020) to 6196 kWh × year (+18.0%), and 6248 kWh × year (+18.7%) by 2050, respectively. The breakdown in heating and cooling needs revealed a divergent trend (see Table 4): the heating energy needs showed a decrease in the order of 129.5% (RCP4.5) and 185.8% (RCP8.5), whereas the cooling energy needs increased by 47.8% (RCP4.5) and 50.3% (RCP8.5).

Table 4. Air temperature (T_{air}), relative humidity (UR), horizontal global solar irradiance ($I_{\text{g,H}}$), heating energy needs ($\varphi_{\text{h,tot}}$), cooling energy needs ($\varphi_{\text{c,tot}}$), peak power for heating ($\varphi_{\text{h,max}}$) and peak power for cooling ($\varphi_{\text{c,max}}$) for the three analyzed scenarios.

Year	T_{air} (°C)	UR (%)	$I_{\text{g,H}}$ (kWh/m ²)	$\varphi_{\text{h,tot}}$ (kWh)	$\varphi_{\text{c,tot}}$ (kWh)	$\varphi_{\text{h,max}}$ (kW)	$\varphi_{\text{c,max}}$ (kW)
2020	15.8	74.4	160.3	2390.7	2688.4	2.5	3.0
2050 (RCP4.5)	19.2	70.1	188.7	1041.8	5153.8	2.0	3.8
2050 (RCP8.5)	19.7	69.0	188.8	836.4	5411.9	1.9	4.0

This trend was reflected in terms of maximum hourly peak power too—that of the heating system dropped from 2.5 kW (2020) to 1.9 kW (RCP8.5), while that of the cooling system rose from 3.0 kW (2020) to 4.0 kW (RCP8.5).

By performing a frequency distribution analysis of hourly energy demand (see Figure 3), an increase of about 6% was shown for the 1–2 kWh (light blue) and 2–3 kWh (blue) cooling ranges for both future scenarios, while a decrease of about 8% was shown for the 1–2 kWh (orange) heating range.

Moreover, for both future scenarios, the 2–3 kWh (red) heating range disappeared and the 3–4 kWh (black) cooling range was introduced due to an increase in outdoor temperature and solar irradiances. Only the heating range 0–1 kWh (yellow) remained unchanged among the different scenarios.

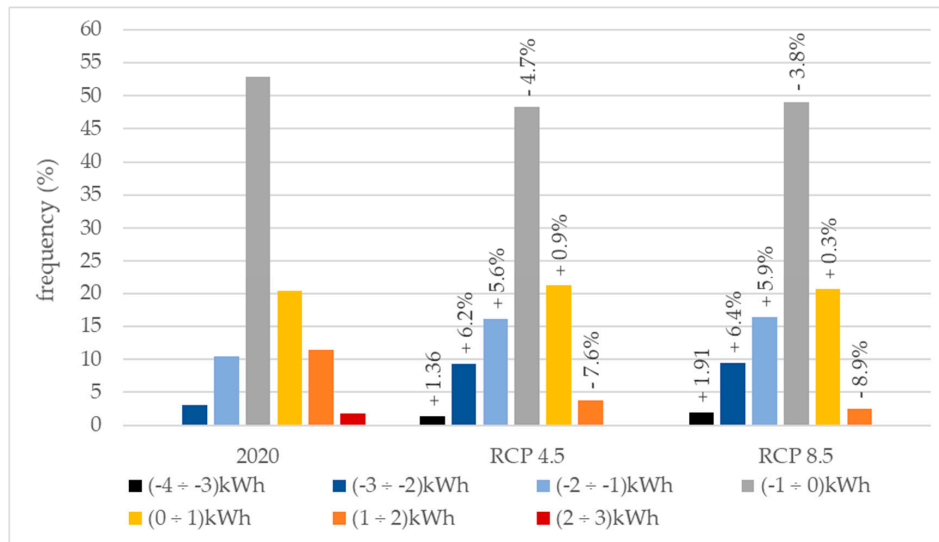


Figure 3. Frequency distribution of energy needs for heating and cooling. Negative ranges refer to cooling, positive to heating.

In addition to the increases in peak power and cooling energy demand, the number of hours over which the cooling system was active increased too—from 3033 h in 2020 to 3983 h (+23.8%) and 4022 h (+24.6%) under RCP4.5 and RCP8.5 scenarios, respectively. Indeed, the length of the cooling season (calculated from the first to the last day the system was on) varied for the different scenarios—174 days in 2020, 224 in 2050 (RCP4.5) and 208 in 2050 (RCP8.5). At the same time, the percentage of hours over which the conditioning system stayed off ($T_{\text{air}} \leq 26 \text{ }^{\circ}\text{C}$) was found to be higher for RCP4.5 than RCP8.5 (25.9% and 19.5%, respectively). Therefore, the number of hours the cooling system was switched on for in the two future scenarios was similar—3983 h for RCP4.5 and 4023 h for RCP8.5.

In combination with the increase in temperature, the model ERA-Interim/UrbClim [42] provides also an increase in global solar irradiance on the horizontal plane ($I_{g,H}$), and thus on tilted and oriented surfaces. As shown in Figure 4, an evident increase in global solar irradiance was observed for both future scenarios compared to 2020, resulting in an increase in solar gains, especially during the months of January, October, November and December. The increase in solar irradiance in the summer months, although greater than in the winter months, did not lead to an evident increase in internal gains. This is because, in order to design an nZEB building, Italian requirements [40] force the use of mobile shading throughout the summer period.

The average annual percentage of global solar irradiance on the horizontal plane was found to increase (see Table 5) by about 19.7% and 15.5% for the cooling period (May–October) and the heating period (November–April), respectively, for both future scenarios. Figure 4 and Table 5 show that the average monthly solar gains do not increase in summer between 2020 and 2050, due to movable shading devices operating in summertime only. Assuming equal internal gains and ventilation rates, the increase in average summer energy consumption, accounting for 249.3% (+2463.4 kWh) and 293.5% (+2723.5 kWh) under RCP4.5 and RCP8.5, respectively, was ascribable to the corresponding average temperature increase (2.7 °C and 3.2 °C). Differently, the decrease in average winter consumption, accounting for 70.3% (−1350.9 kWh) and 77.0% (−1554.3 kWh) under RCP4.5 and RCP8.5, respectively, was associated with both the average increase in temperature (2.1 °C and 2.5 °C) and the increase in solar radiation.

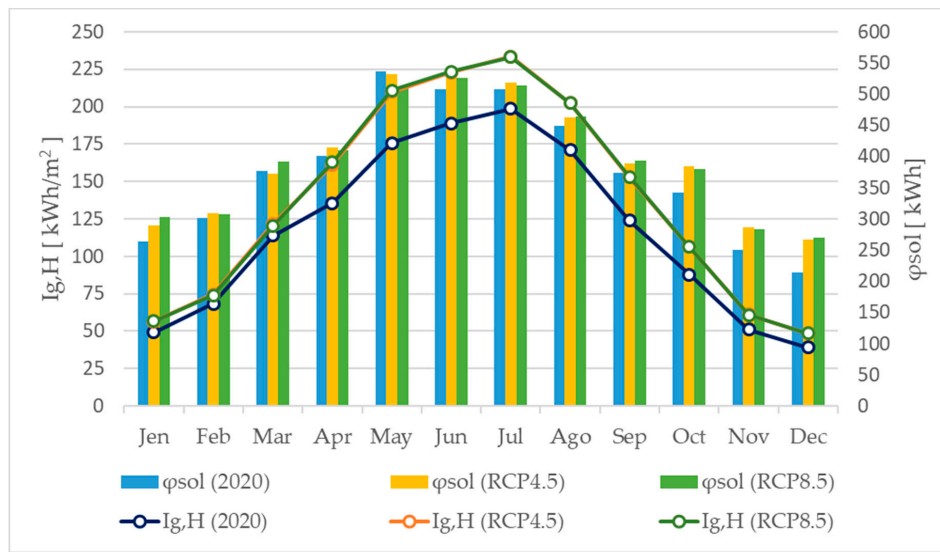


Figure 4. Monthly sum of solar gains (φ_{sol}) and solar global irradiance on the horizontal plane ($I_{g,H}$) for 2020, 2050 (RCP4.5) and 2050 (RCP8.5).

Table 5. Monthly percentage variation of the main input and output values between 2020 and the RCP4.5 and RCP8.5 (2050) scenarios.

2020 vs. 2050 (RCP4.5)						2020 vs. 2050 (RCP8.5)					
Mtly	T _{air}	I _{g,H}	φ _{sol}	φ _h	φ _c	Mtly	T _{air}	I _{g,H}	φ _{sol}	φ _h	φ _c
Jen	54.2%	14.3%	9.4%	-54.2%	-	Jen	58.8%	15.5%	14.8%	-59.2%	-
Feb	38.2%	9.3%	2.6%	-48.2%	-	Feb	46.0%	8.2%	1.8%	-58.3%	-
Mar	24.4%	6.9%	-1.3%	-68.4%	-	Mar	27.8%	5.7%	4.0%	-78.1%	-
Apr	26.1%	18.9%	3.6%	-100.0%	-	Apr	26.6%	20.0%	2.3%	-100.0%	-
May	15.3%	19.6%	-0.7%	-	160.8%	May	16.3%	20.1%	-4.7%	-	157.2%
Jun	15.3%	18.0%	4.8%	-	69.6%	Jun	16.9%	18.3%	3.6%	-	74.9%
Jul	19.7%	17.5%	1.9%	-	64.1%	Jul	22.4%	17.3%	1.2%	-	71.9%
Ago	21.2%	18.2%	2.8%	-	75.4%	Ago	23.7%	18.2%	3.3%	-	84.9%
Sep	19.8%	23.4%	3.8%	-	160.9%	Sep	22.5%	23.5%	4.9%	-	184.1%
Oct	15.2%	21.3%	12.2%	-	964.6%	Oct	18.6%	20.9%	10.8%	-	1187.8%
Nov	20.9%	19.7%	14.2%	-95.8%	-	Nov	25.3%	19.5%	12.8%	-100.0%	-
Dec	33.0%	24.0%	24.1%	-55.0%	-	Dec	38.8%	24.2%	25.9%	-66.7%	-

By performing a non-linear regression analysis between daily heating/cooling needs and outdoor air temperatures (see Figure 5), we observed how future distributions gradually shift towards higher temperatures and consumptions—from a maximum cooling demand of 40.4 kWh/day in 2020 to 64.3 kWh/day under RCP4.5 and 68.0 kWh/day under RCP8.5. Precisely for this reason, the distribution in graphs b and c of Figure 5 loses symmetry, and the density of the points in the left side (heating needs) decreases. Figure 5 also shows that the minima ($\varphi_{h/c} = 0$) of the trendlines for future scenarios (graph b and c) narrow down and get slightly shifted towards higher temperatures (to 16.0 °C and 16.5 °C, respectively), compared to the current scenario (graph a) where 0 $\varphi_{h/c}$ conditions occur between 14.5 °C and 16.6 °C.

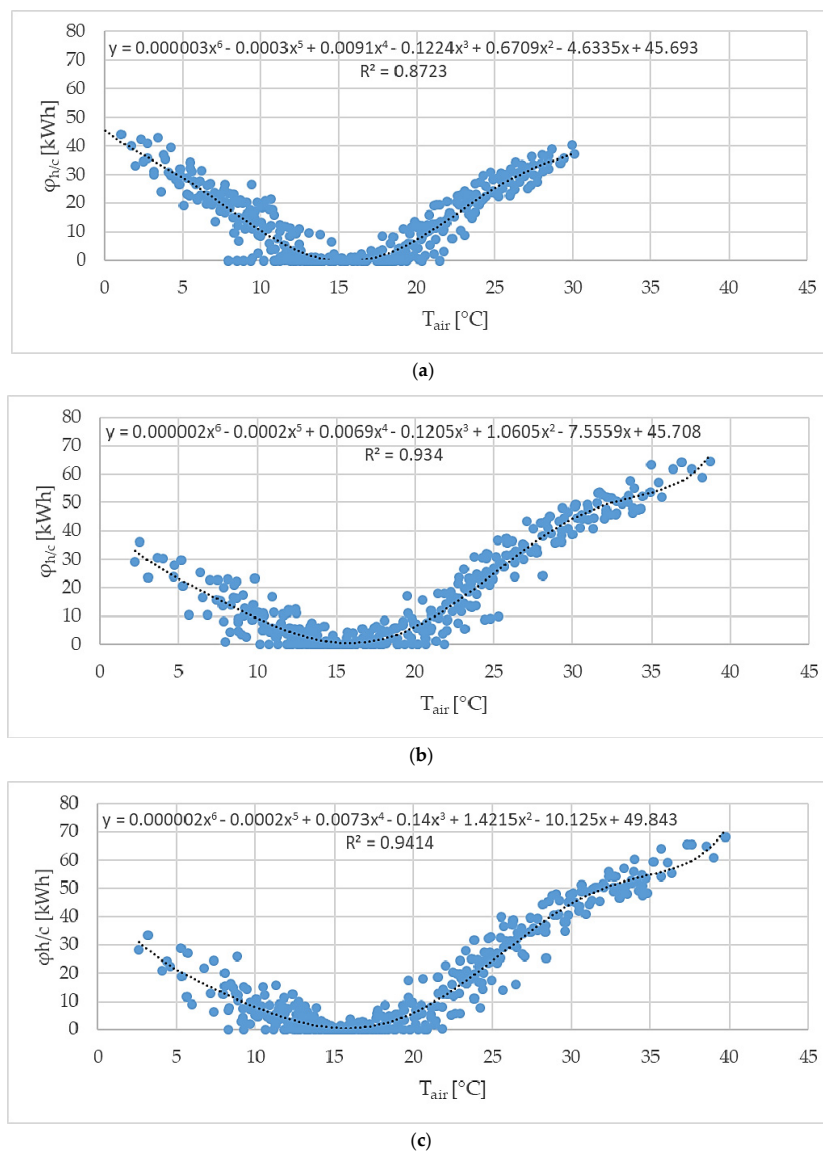


Figure 5. Non-linear regression between daily energy demand of the building and outdoor air temperature: (a) 2020 current scenario, (b) future scenario 2050 RCP4.5 and (c) future scenario 2050 RCP8.5. Trendlines, respective polynomial equations and R-squares are reported on each graph.

3.2. Simulations to Assess Thermal Comfort

In this section, the two approaches employed for the assessment of indoor thermal comfort are sequentially presented: (i) the adaptive method and (ii) the combined long-term index proposed by Li et al. [49].

The assessment of adaptive comfort can be performed only on buildings used mainly for human occupancy engaged in sedentary activities (e.g., residential buildings and offices), where thermal conditions can be regulated by occupants through accessing operable windows and adapting their behavior. On the other hand, the new combined index considers the long-term thermal satisfaction in response to pronounced excursions and daily variability.

The analysis was performed for two rooms (see Figure 6), one due southeast (living room) and one due northwest (double bedroom), to account for different exposures and thus different solar gains. The evaluation focused on the cooling periods as identified in Section 3.1 (174 days in 2020, 224 in 2050 (RCP4.5) and 208 in 2050 (RCP8.5)); therefore, the assessment of thermal comfort is performed for each climate scenario over different periods, assuming the absence of cooling systems.

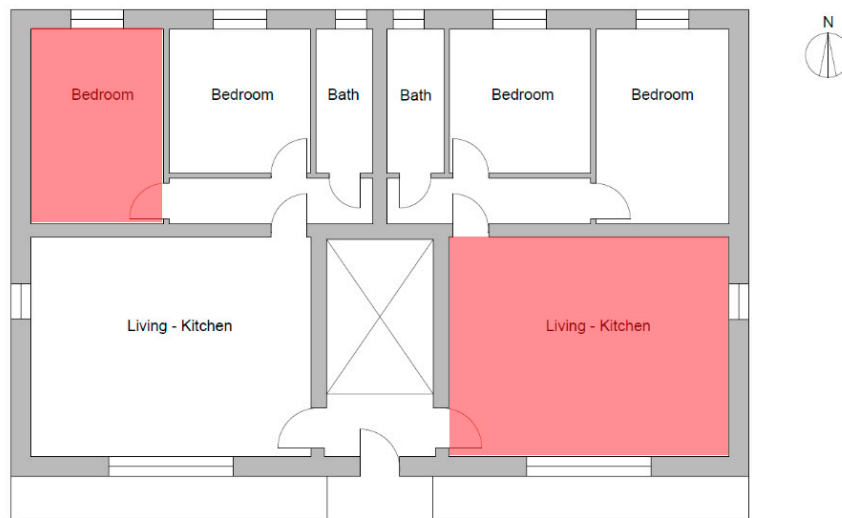


Figure 6. Representative rooms for adaptive comfort assessment: southeast living room and northwest double bedroom.

Regarding the adaptive method, as shown in Table 6, the living room provided comfort conditions (operative temperature cooling set point of 26 °C) for shorter time periods than the double bedroom, regardless of the scenario. Assuming category II as a reference, the percent decrease between 2020 and 2050 RCP4.5 reached 4.1% and 3.7% for the two considered rooms, against 9.0% for both rooms under RCP8.5.

Table 6. Adaptive comfort assessment for the two analyzed rooms under different climate scenarios: comfort hours and percentages over the relevant cooling periods.

Year	Cooling Period			Room	Cat. I		Cat. II		Cat. III	
	Data	Days	h		h	%	h	%	h	%
2020	6 May–26 October	174	4176	Living room	681	16.3%	1091	26.1%	1566	37.5%
				Bedroom	1266	30.3%	1883	45.1%	2169	51.9%
2050 (RCP4.5)	6 April–15 November	224	5376	Living room	733	13.6%	1186	22.1%	1788	33.3%
				Bedroom	1840	34.2%	2223	41.4%	2422	45.1%
2050 (RCP8.5)	6 April–30 October	208	4992	Living room	513	10.3%	855	17.1%	1299	26.0%
				Bedroom	1184	23.7%	1800	36.1%	2035	40.8%

Results for the combined index are shown in Table 7. The double bedroom experienced percent increases in discomfort events of 0.9% and 3.6% between 2020 and 2050 for RCP4.5 and RCP8.5, respectively. In contrast, for the living room the variation stayed below 1% under both the considered scenarios.

Table 7. Combined index assessment for the two analyzed rooms under different climatic scenarios: percentages over the relevant cooling periods.

Year	Cooling Period			Room	Combined Discomfort Index
	Data	Days	h		%
2020	26 May–26 October	174	4176	Living room	56.1%
				Bedroom	47.9%
2050 (RCP4.5)	6 April–15 November	224	5376	Living room	55.0%
				Bedroom	48.8%
2050 (RCP8.5)	6 April–30 October	208	4992	Living room	55.9%
				Bedroom	51.5%

4. Discussion and Conclusions

The global climate is undergoing major upheavals, posing a serious risk of premature obsolescence for the current nZEB paradigms.

In accordance with the experimental study by A. Martinelli et al. [56], wherein it is shown that the Urban Heat Island phenomenon is more accentuated in the areas closer to the city center, the ERA-Interim/CliUrbm predictive model [42,43] used in this study identified Rome as the Italian city that will undergo the greatest temperature increase by 2050. For this reason, the impact of climate change on the energy needs and indoor comfort of an nZEB located in this location was assessed.

Based on the simulations made and detailed in Sections 2 and 3, the following considerations can be made:

The respective rises of 3.4 °C and 3.9 °C by 2050 for the RCP4.5 and RCP8.5 scenarios do not lead to decreases in heating needs great enough to meet the sharp increase in cooling needs. Specifically, in fact, compared to the current energy needs, there will be an average annual increase of 1143 kWh (+22.4%). This increase is consistent with the increase obtained by Ciancio et al. [4] (+34.4%) for the building located in Rome, which is not an nZEB, but has similar transmittances to our case study.

- a. Peak electricity demand is especially worrisome since it is usually covered by low-efficiency power plants, yet it is strongly associated with typical nZEB paradigms. In fact, while air conditioning is only a fraction of all building energy uses, it is the primary driver of peak electricity demand [57]. Efficiently curbing the air conditioning needs by targeting a resilient nZEB design will be key in the future.
- b. According to the ERA-Interim/UrbClim model, by 2050, not only will temperatures rise, but a 19.7% increase in global solar irradiance on the horizontal plane is also to be expected during the summer months, thus triggering higher solar gains. The increase in the solar irradiance, often underestimated by the models [58,59], is consistent with the study conducted by M. Wild et al. [60], which predicts a decrease in solar radiation (clear-sky condition) for many regions of the world, except for parts of China and Europe. In our case study, the increase in the solar irradiance does not imply an increase in the solar contributions inside the building because the national nZEB regulation foresees the use of mobile shading devices for the whole summer period. These systems appear rather effective, since the increase in solar gains is negligible in summer, but becomes evident in winter (particularly in January, October, November and December).
- c. By performing simulations in the absence of cooling systems, 6.2% and 5.1% reductions in the hours of adaptive comfort are determined under the RCP4.5 (2050) and RCP8.5 (2050) scenarios, respectively, out of the concerted actions of temperature and solar gains. The results of the newly proposed combined index for long-term comfort assessments revealed a milder future penalty. The index estimates how the level of occupant adaptation and sensitivity to variation would be affected in the future. It was demonstrated that the comfort implications of the pronounced excursions and large variations in daily temperature will be marginal under both scenarios, with greater influence on northwest rather than southeast oriented thermal zones, likely owing to the effect of the combination of higher temperatures and higher solar irradiation in levelling out the daily swings.

In conclusion, this study adds to the current body of knowledge on the preservation of nZEB performance in the future by performing hourly dynamic simulations on a reference building in Rome, modeled in accordance with the latest legislations. It quantifies potential changes in terms of energy and comfort levels and provides useful recommendations to legislators on building standards, both for the design of new nZEBs, e.g., the presence of solar shading devices, and for the renovation of the existing building stock. Further analysis may target climate dependencies and may include technological variants.

Author Contributions: Conceptualization, S.S. and L.T.; methodology, S.S., L.T., G.U. and C.D.P.; software, L.T.; validation, S.S.; formal analysis, S.S.; investigation, S.S.; resources, S.S.; data curation S.S.; writing—original draft preparation, S.S.; writing—review and editing, S.S., L.T. and G.U.; visualization, S.S., L.T. and C.D.P.; supervision, C.D.P. All authors have read and agreed to the published version of the manuscript.

Funding: This research received no external funding.

Conflicts of Interest: The authors declare no conflict of interest.

References

- Lucon, O.; Urge-Vorsatz, D.; Ahmed, A.Z.; Akbari, H.; Bertoldi, P.; Cabeza, L.F.; Liphoto, E. Gadgil Chapter 9—Buildings. In *Climate Change 2014: Mitigation of Climate Change. IPCC Working Group III Contribution to AR5*; Cambridge University: Cambridge, UK, 2014.
- Urge-Vorsatz, D.; Lucon, O.; Zain Ahmed, A.; Akbari, H.; Bertoldi, P.; Cabeza, L.F.; Eyre, N.; Gadgil, A.; Harvey, L.D.D.; Jiang, Y.; et al. Buildings. In *Mitigation. Working Group III contribution to the Fifth Assessment Report of the Intergovernmental Panel of Climate Change*; Cambridge University: Cambridge, UK, 2014; pp. 671–738.
- IPCC. *Climate Change—The Synthesis Report*; IPCC: Geneva, Switzerland, 2014.
- Ciancio, V.; Salata, F.; Falasca, S.; Curci, G.; Golasi, I.; de Wilde, P. Energy demands of buildings in the framework of climate change: An investigation across Europe. *Sustain. Cities Soc.* **2020**, *60*, 102213. [[CrossRef](#)]
- Olonscheck, M.; Holsten, A.; Kropp, J.P. Heating and cooling energy demand and related emissions of the German residential building stock under climate change. *Energy Policy* **2011**, *39*, 4795–4806. [[CrossRef](#)]
- Verichev, K.; Zamorano, M.; Carpio, M. Effects of climate change on variations in climatic zones and heating energy consumption of residential buildings in the southern Chile. *Energy Build.* **2020**, *215*, 109874. [[CrossRef](#)]
- Angeles, M.E.; González, J.E.; Ramírez, N. Impacts of climate change on building energy demands in the intra-Americas region. *Theor. Appl. Climatol.* **2018**, *133*, 59–72. [[CrossRef](#)]
- Frank, T. Climate change impacts on building heating and cooling energy demand in Switzerland. *Energy Build.* **2005**, *37*, 1175–1185. [[CrossRef](#)]
- Tribuiani, C.; Tarabelli, L.; Summa, S.; Di Perna, C. Thermal performance of a massive wall in the Mediterranean climate: Experimental and analytical research. *Appl. Sci.* **2020**, *10*, 4611. [[CrossRef](#)]
- Cabeza, L.F.; Chàfer, M. Technological options and strategies towards zero energy buildings contributing to climate change mitigation: A systematic review. *Energy Build.* **2020**, *219*, 110009. [[CrossRef](#)]
- Ulpiani, G.; Summa, S.; di Perna, C. Sunspace coupling with hyper-insulated buildings: Investigation of the benefits of heat recovery via controlled mechanical ventilation. *Sol. Energy* **2019**, *181*, 17–26. [[CrossRef](#)]
- Troup, L.; Eckelman, M.J.; Fannon, D. Simulating future energy consumption in office buildings using an ensemble of morphed climate data. *Appl. Energy* **2019**, *255*, 113821. [[CrossRef](#)]
- Wang, L.; Liu, X.; Brown, H. Prediction of the impacts of climate change on energy consumption for a medium-size office building with two climate models. *Energy Build.* **2017**, *157*, 218–226. [[CrossRef](#)]
- Favaro, P.A.; Manz, H. Temperature-driven single-sided ventilation through a large rectangular opening. *Build. Environ.* **2005**, *40*, 689–699. [[CrossRef](#)]
- Petcu, C.; Petran, H.-A.; Vasile, V.; Toderasc, M.-C. Materials from Renewable Sources as Thermal Insulation for Nearly Zero Energy Buildings (nZEB). In *Conference on Sustainable Energy*; Springer: Cham, Switzerland, 2017; pp. 159–167.
- Carmo, C.; Dumont, O.; Nielsen, M.P.; Elmegaard, B. Assessment of Emerging Renewable Energy-based Cogeneration Systems for nZEB Residential Buildings. *Environ. Sci. Eng.* **2016**.
- De Santoli, L.; Basso, G.L.; Spiridigliozzi, G.; Garcia, D.A. Innovative Hybrid Energy Systems for Heading Towards NZEB Qualification for Existing Buildings. In *Proceedings of the 2018 IEEE International Conference on Environment and Electrical Engineering and 2018 IEEE Industrial and Commercial Power Systems Europe (EEEIC/I&CPS Europe)*; Institute of Electrical and Electronics Engineers (IEEE): New York, NY, USA, 2018; pp. 1–6. [[CrossRef](#)]
- Stritih, U.; Tyagi, V.V.; Stropnik, R.; Paksoy, H.; Haghighat, F.; Joybari, M.M. Integration of passive PCM technologies for net-zero energy buildings. *Sustain. Cities Soc.* **2018**, *41*, 286–295. [[CrossRef](#)]

19. Georgiou, G.S.; Christodoulides, P.; Kalogirou, S.A. Optimizing the energy storage schedule of a battery in a PV grid-connected nZEB using linear programming. *Energy* **2020**, *208*, 118177. [[CrossRef](#)]
20. Kazmi, H.; D'Oca, S.; Delmastro, C.; Lodeweyckx, S.; Corgnati, S.P. Generalizable occupant-driven optimization model for domestic hot water production in NZEB. *Appl. Energy* **2016**, *175*, 1–15. [[CrossRef](#)]
21. Wemhoener, C.; Schwarz, R.; Rominger, L. IEA HPT Annex 49-Design and integration of heat pumps in nZEB. *Energy Procedia* **2017**, *122*, 661–666. [[CrossRef](#)]
22. Gondal, I.A. Prospects of Shallow geothermal systems in HVAC for NZEB. *Energy Built Environ.* **2020**. [[CrossRef](#)]
23. Becchio, C.; Corgnati, S.P.; Vio, M.; Crespi, G.; Prendin, L.; Ranieri, M.; Vidotto, D. Toward NZEB by optimizing HVAC system configuration in different climates. *Energy Procedia* **2017**, *140*, 115–126. [[CrossRef](#)]
24. Kim, D.; Cho, H.; Koh, J.; Im, P. Net-zero energy building design and life-cycle cost analysis with air-source variable refrigerant flow and distributed photovoltaic systems. *Renew. Sustain. Energy Rev.* **2020**, *118*, 109508. [[CrossRef](#)]
25. Naveen Chakkaravarthy, A.; Subathra, M.S.P.; Jerin Pradeep, P.; Manoj Kumar, N. Solar irradiance forecasting and energy optimization for achieving nearly net zero energy building. *J. Renew. Sustain. Energy* **2018**, *10*, 035103. [[CrossRef](#)]
26. Reda, F.; Fatima, Z. Northern European nearly zero energy building concepts for apartment buildings using integrated solar technologies and dynamic occupancy profile: Focus on Finland and other Northern European countries. *Appl. Energy* **2019**, *237*, 598–617. [[CrossRef](#)]
27. Synnefa, A.; Laskari, M.; Gupta, R.; Pisello, A.L.; Santamouris, M. Development of Net Zero Energy Settlements Using Advanced Energy Technologies. *Procedia Eng.* **2017**, *180*, 1388–1401. [[CrossRef](#)]
28. Gholami, H.; Nils Røstvik, H.; Manoj Kumar, N.; Chopra, S.S. Lifecycle cost analysis (LCCA) of tailor-made building integrated photovoltaics (BIPV) façade: Solsmaragden case study in Norway. *Sol. Energy* **2020**, *211*, 488–502. [[CrossRef](#)]
29. Pikas, E.; Kurnitski, J.; Thalfeldt, M.; Koskela, L. Cost-benefit analysis of nZEB energy efficiency strategies with on-site photovoltaic generation. *Energy* **2017**, *128*, 291–301. [[CrossRef](#)]
30. European Community (EC). Directive (EU) 2018/844 of the European Parliament and of the Council of 30 May 2018 Amending Directive 2010/31/EU on the Energy Performance of Buildings Directive 2012/27/EU on Energy Efficiency; L156/75. In *Official Journal of the European Union*; European Union: Brussels, Belgium, 2018.
31. Karlessi, T.; Kampelis, N.; Kolokotsa, D.; Santamouris, M.; Standardi, L.; Isidori, D.; Cristalli, C. The Concept of Smart and NZEB Buildings and the Integrated Design Approach. *Procedia Eng.* **2017**, *180*, 1316–1325. [[CrossRef](#)]
32. Rey-Hernández, J.M.; González, S.L.; San José-Alonso, J.F.; Tejero-González, A.; Velasco-Gómez, E.; Rey-Martínez, F.J. Smart energy management of combined ventilation systems in a nZEB. *E3S Web Conf.* **2019**, *111*. [[CrossRef](#)]
33. Ulpiani, G.; Ranzi, G.; Bruederlin, F.; Paolini, R.; Fiorito, F.; Haddad, S.; Kohl, M.; Santamouris, M. Elastocaloric cooling: Roadmap towards successful implementation in the built environment. *AIMS Mater. Sci.* **2019**, *6*, 1135–1152. [[CrossRef](#)]
34. Ulpiani, G.; Ranzi, G.; Shah, K.W.; Feng, J.; Santamouris, M. On the energy modulation of daytime radiative coolers: A review on infrared emissivity dynamic switch against overcooling. *Sol. Energy* **2020**, *209*, 278–301. [[CrossRef](#)]
35. Harkouss, F.; Fardoun, F.; Biwolé, P.H. Optimization approaches and climates investigations in NZEB—A review. *Build. Simul.* **2018**, *11*, 923–952. [[CrossRef](#)]
36. Feng, W.; Zhang, Q.; Ji, H.; Wang, R.; Zhou, N.; Ye, Q.; Hao, B.; Li, Y.; Luo, D.; Lau, S.S.Y. A review of net zero energy buildings in hot and humid climates: Experience learned from 34 case study buildings. *Renew. Sustain. Energy Rev.* **2019**, *114*, 109303. [[CrossRef](#)]
37. Di Giuseppe, E.; Ulpiani, G.; Summa, S.; Tarabelli, L.; Di Perna, C.; D'Orazio, M. Hourly dynamic and monthly semi-stationary calculation methods applied to nZEBs: Impacts on energy and comfort. *IOP Conf. Ser. Mater. Sci. Eng.* **2019**, *609*, 072008. [[CrossRef](#)]

38. International Organization for Standardization. *Energy Performance of Buildings—Energy Needs for Heating and Cooling, Internal Temperatures and Sensible and Latent Heat Loads—Part 1: Calculation Procedures*; International Organization for Standardization: Geneva, Switzerland, 2017; p. 204.
39. CEN European Committee for Standardization. *EN ISO 13790: 2008 Energy Performance of Buildings—Calculation of Energy Use for Space Heating and Cooling*; European Committee for Standardization: Brussels, Belgium, 2008.
40. Italian Republic. *Italian Interministerial Decree 26th June 2015: Application of Calculation Methods for Energy Performance and Definition of Minimum Building Requirements*; Ministry of Economic Development: Roma, Italy, 2015; pp. 1–8.
41. World Climate Research Program. EURO-CORDEX—Coordinated Downscaling Experiment—European Domain. Available online: <https://euro-cordex.net/> (accessed on 28 October 2020).
42. Flemish Research & Technology Organisation VITO. Urban Climate Service Centre. Available online: www.urban-climate.be (accessed on 28 October 2020).
43. Remund, J.; Grossenbacher, U. Urban Climate-Impact on Energy Consumption and Thermal Comfort of Buildings Urban Climate—Impact on Energy Consumption and Thermal Comfort of Buildings. In Proceedings of the International Conference on Solar Energy for Buildings and Industry EuroSun2018, Rapperswil, Switzerland, 10–13 September 2018. [CrossRef]
44. Duffy, M.J.; Hiller, M.; Bradley, D.E.; Keilholz, W.; Thornton, J.W. TRNSYS-features and functionality for building simulation 2009 conference. In Proceedings of the 11th International IBPSA Conference-Building Simulation, Glasgow, UK, 27–30 July 2009; pp. 1950–1954.
45. Crawley, D.B.; Hand, J.W.; Kummert, M.; Griffith, B.T. Contrasting the capabilities of building energy performance simulation programs. *Build. Environ.* **2008**, *43*, 661–673. [CrossRef]
46. Vadiée, A.; Dodo, A.; Gustavsson, L. A Comparison Between Four Dynamic Energy Modeling Tools for Simulation of Space Heating Demand of Buildings. In *Cold Climate HVAC Conference*; Springer: Cham, Switzerland, 2019; pp. 701–711. [CrossRef]
47. Duffy, M.J.; Hiller, M.; Bradley, D.E.; Keilholz, J.W.W. *TRNSYS 17: A Transient System Simulation Program*; Solar Energy Laboratory, University of Wisconsin: Madison, WI, USA, 2010.
48. CEN European Committee for Standardization. *EN 16798-1:2019 Energy Performance of Buildings—Ventilation for Buildings—Part 1: Indoor Environmental Input Parameters for Design and Assessment of Energy Performance of Buildings Addressing Indoor Air Quality, Thermal Environment, Lighting and Acous*; European Committee for Standardization: Brussels, Belgium, 2019.
49. Li, P.; Parkinson, T.; Schiavon, S.; Froese, T.M.; de Dear, R.; Rysanek, A.; Staub-French, S. Improved long-term thermal comfort indices for continuous monitoring. *Energy Build.* **2020**, *224*, 110270. [CrossRef]
50. Meteotest. *Meteonorm 7 V7.3.3*; Meteotest: Bern, Switzerland, 2018.
51. Remund, J.; Müller, S.; Studer, C.; Cattin, R. *Handbook Part II: Theory Global Meteorological Database Version 7 Software and Data for Engineers, Planners and Education. Handbook Part II: Theory*; Meteotest AG: Bern, Switzerland, 2019.
52. Giorgi, F.; Jones, C.; Asrar, G.R. Addressing climate information needs at the regional level: The CORDEX framework. *WMO Bull.* **2009**, *58*, 175–183.
53. Trimble, I.N.C. SketchUp. 2020. Available online: <https://www.sketchup.com/node/4481> (accessed on 28 October 2020).
54. Ellis, P. OpenStudio Plugin for Google SketchUp3D. 2009. Available online: <https://www.openstudio.net/> (accessed on 28 October 2020).
55. UNI-Ente Italiano di Normazione, UNI/TS 11300-1:2014-*Energy Performance of Buildings-Part 1: Evaluation of Energy Need for Space Heating and Cooling*; Comitato Termotecnico Italiano (CTI): Milan, Italy, 2014.
56. Martinelli, A.; Kolokotsa, D.D.; Fiorito, F. Urban heat island in Mediterranean coastal cities: The case of Bari (Italy). *Climate* **2020**, *8*, 79. [CrossRef]
57. Ortiz, L.; González, J.E.; Lin, W. Climate change impacts on peak building cooling energy demand in a coastal megacity. *Environ. Res. Lett.* **2018**, *13*, 094008. [CrossRef]
58. Allen, R.J.; Norris, J.R.; Wild, M. Evaluation of multidecadal variability in CMIP5 surface solar radiation and inferred underestimation of aerosol direct effects over Europe, China, Japan, and India. *J. Geophys. Res. Atmos.* **2013**, *118*, 6311–6336. [CrossRef]

59. Wild, M.; Schmucki, E. Assessment of global dimming and brightening in IPCC-AR4/CMIP3 models and ERA40. *Clim. Dyn.* **2011**, *37*, 1671–1688. [[CrossRef](#)]
60. Wild, M.; Folini, D.; Henschel, F.; Fischer, N.; Müller, B. Projections of long-term changes in solar radiation based on CMIP5 climate models and their influence on energy yields of photovoltaic systems. *Sol. Energy* **2015**, *116*, 12–24. [[CrossRef](#)]

Publisher's Note: MDPI stays neutral with regard to jurisdictional claims in published maps and institutional affiliations.



© 2020 by the authors. Licensee MDPI, Basel, Switzerland. This article is an open access article distributed under the terms and conditions of the Creative Commons Attribution (CC BY) license (<http://creativecommons.org/licenses/by/4.0/>).